16-Channel Parallel Transmission in the Human Brain at 9.4 Tesla: Initial Results

X. Wu[1], **J. T. Vaughan**[1], **K. Ugurbil**[1], **and P-F. Van de Moortele**[1]
[1]CMRR, University of Minnesota, Minneapolis, MN, United States

Introduction: It has been shown that parallel transmission (pTx) [1-5], which consists of playing different RF pulses through independent transmit (Tx) channels, can be used to mitigate Tx B1 (B1+) nonuniformity and to achieve more homogeneous spatially selective RF excitation at high magnetic field. At this time, human scanners equipped with a Multi Tx console have typically a much smaller number of Tx channels than Receive (Rx) channels (8 Tx channels is probably the most common case). There is however a growing body of evidence suggesting that better performance are expected when using a larger number of Tx channels [6,7]. We have previously reported a successful implementation of Transmit SENSE in the human brain at 9.4 T with an 8 Tx channel system, which required addressing methodological issues such as k-space trajectory inaccuracies and large susceptibility induced ΔB0 [8]. Recently, our 9.4T system has been upgraded with a 16 Tx channel console. Here we report preliminary results of 2D (Transmit SENSE) and 3D (Spoke trajectories) pTx in the human brain at 9.4 T using a 16-channel RF coil.

Materials and Methods: All experiments were conducted on a 9.4 T human scanner (Magnex, UK) driven by a console with 16 independent Tx RF channels (Varian, USA), each powered with a 500 W RF amplifier (CPC, USA). A 16-ch transceiver strip-line array [9] was used for both transmission and reception. Healthy volunteers were recruited for this study. All computations were performed in Matlab. In-vivo B1+ maps (Fig. 1) were obtained for individual channels using a fast multi-channel B1+ mapping technique [10]. ΔB_0 maps were derived from images acquired at two TE and were incorporated into RF pulse design to minimize off-resonance effects. All pTx RF pulses were designed in small tip angle regime using the spatial domain method [4]. For 2D pTx experiments, RF pulses were calculated with a slew rate-limited spiral trajectory undersampling the k-space by a factor of 4 (~2.4 ms in length). Two target excitation patterns were considered in an axial slice of the brain (a rectangle and a logo "M"). The minimization problem was solved with conjugate gradient iterations. To correct for excitation distortions due to gradient errors, the actually measured k-space trajectory was used for pulse design [8]. Excitation patterns were imaged using a modified 3D gradient echo (GE) pulse. For 3D pTx experiments, slice-selective RF pulses were designed using a 5-spoke trajectory to mitigate B1+ inhomogeneity and achieve a more uniform excitation. The spoke placement was determined based on the Fourier transform (FT) of the desired in-plane uniform excitation. Spokes were placed where the 5 largest FT coefficients were found. Subpulses were Gaussian shaped with a time-bandwidth-product of 2. Slice-selective gradients were designed for a slice thickness of 5 mm. The total pulse duration was 4.5 ms (without the gradient rewinder). The complex weights corresponding to each spoke and to each coil element were calculated using a magnitude least squares optimization [5] where the Tikhonov regularization parameter was determined by the L-curve criterion [3]. The k-space deviation existing on our system was ignored in 3D pTx pulse design since our preliminary simulation shows insensitivity of 3D pulses to gradient errors. The resulting RF pulse for one channel and gradient waveforms are shown in Fig. 2. The in-plane excitation pattern was imaged with a modified 2D GE pulse sequence. All data shown here were normalized by the estimated product [Proton Density] × [Receive B1 profile] (ρ|B1-|) in order to better identify the Tx B1 component.

Results and Discussion: Fig. 3 shows experimental excitation patterns for 2D pTx RF pulses designed with the measured k-space trajectory. The excitation patterns matched the target patterns, although some brain structures were visible. This is mostly due to residual T1 weight present in the brain images used for estimating ρ|B1-| (long T1's are observed in brain tissues at 9.4 T). Fig. 4 displays the excitation pattern (left) along with six intensity profiles (right) corresponding to the red dotted lines (left) for slice selective 3D pTx pulses. Overall B1+ homogeneity was satisfactory through the slice of interest, but one can notice that some areas of weak signals were still present. Our preliminary investigations suggest that these residual inaccuracies, which are not observed in our 2D Transmit SENSE results, may reflect a high sensitivity of these 3D pTx RF pulses to eddy currents that are not directly measured with our k-space trajectory sampling method. This could especially concern B0 (or higher order) eddy currents induced by the Z axis gradient rapidly switching during the 3D spoke trajectories. By contrast, Z axis gradient is not used during our Transmit SENSE RF pulses as all our excitation targets are defined in an axial view (XY plane).

Conclusions: In this study, preliminary results have been presented for in-vivo 2D and 3D parallel transmission at 9.4 T using a 16-element coil. These initial results are very promising, especially with 2D pTx, while additional calibrations may be required, especially with regards to eddy currents, to obtain more homogeneous 3D pTx excitation patterns.

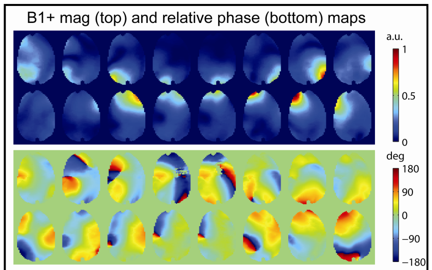

Fig. 1. Tx B1 map for a 16-ch transceiver coil.

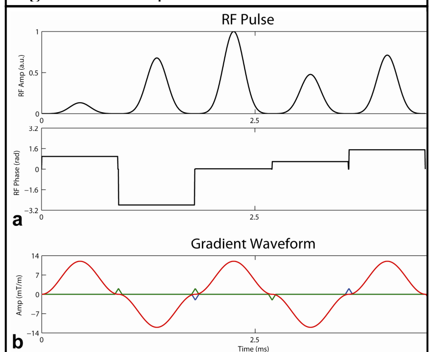

Fig. 2. RF and gradient pulses for 3D pTx. **a:** RF magnitude (top) and phase (bottom) for one channel. **b:** Gx (green), Gy (blue) and Gz (red).

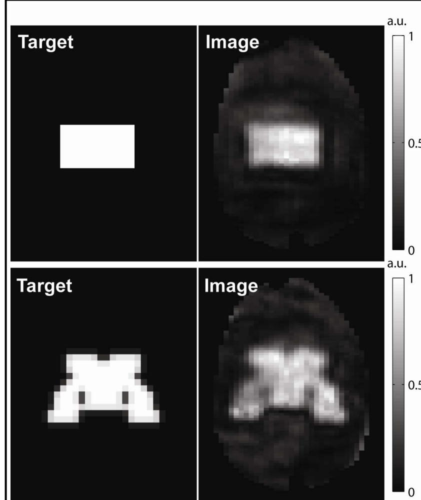

Fig. 3. Results of 2D pTx experiment.

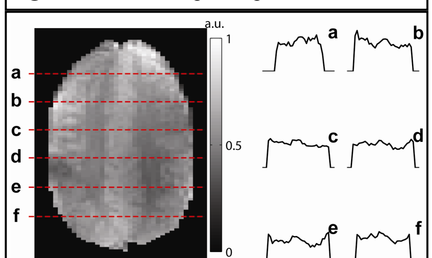

Fig. 4. Results of 3D pTx experiment.

References: **1**. Katscher et al., MRM 49:144-50(2003). **2**. Zhu, MRM 51:775-84(2004). **3**. Ullman et al., MRM 54:994-1001(2005). **4**. Grissom et al., MRM 56:620-629(2006). **5**. Setsompop et al., MRM 59:908-915(2008). **6.** Wu et al., ISMRM 2007, p 3350. **7**. Lattanzi et al., MRM 61:315-334(2009). **8.** Wu et al., MRM, in press. **9.** Adriany et al., ISMRM 2009, p 3005. **10.** Van de Moortele et al., ISMRM 2007, p 1676.

Acknowledgments: KECK Foundation. NIH: EB006835, PAR-02-010, EB007327, P41 RR008079 and P30 NS057091.